Cellular/Molecular

Activity-Dependent Ubiquitination of $GABA_A$ Receptors Regulates Their Accumulation at Synaptic Sites

Richard S. Saliba,[1,2] Guido Michels,[1,3] Tija C. Jacob,[1] Menelas N. Pangalos,[4] and Stephen J. Moss[1,2]

[1]Department of Neuroscience, University of Pennsylvania, Philadelphia, Pennsylvania 19104, [2]Department of Pharmacology, University College London, London WC1E 6BT, United Kingdom, [3]Department of Internal Medicine III, University of Cologne, 50937 Cologne, Germany, and [4]Wyeth Research, Neuroscience Discovery, Princeton, New Jersey 08852

$GABA_A$ receptors ($GABA_A$Rs) are the major mediators of fast synaptic inhibition in the brain. In neurons, these receptors undergo significant rates of endocytosis and exocytosis, processes that regulate both their accumulation at synaptic sites and the efficacy of synaptic inhibition. Here we have evaluated the role that neuronal activity plays in regulating the residence time of $GABA_A$Rs on the plasma membrane and their targeting to synapses. Chronic blockade of neuronal activity dramatically increases the level of the $GABA_A$R ubiquitination, decreasing their cell surface stability via a mechanism dependent on the activity of the proteasome. Coincident with this loss of cell surface expression levels, TTX treatment reduced both the amplitude and frequency of miniature inhibitory synaptic currents. Conversely, increasing the level of neuronal activity decreases $GABA_A$R ubiquitination enhancing their stability on the plasma membrane. Activity-dependent ubiquitination primarily acts to reduce $GABA_A$R stability within the endoplasmic reticulum and, thereby, their insertion into the plasma membrane and subsequent accumulation at synaptic sites. Thus, activity-dependent ubiquitination of $GABA_A$Rs and their subsequent proteasomal degradation may represent a potent mechanism to regulate the efficacy of synaptic inhibition and may also contribute to homeostatic synaptic plasticity.

Key words: **$GABA_A$ receptor; ubiquitination; synapse; proteasome; membrane insertion; inhibition**

Introduction

$GABA_A$ receptors ($GABA_A$Rs), mediate the majority of fast synaptic inhibition in the brain and also represent the major sites of action for both benzodiazepines and barbiturates. These receptors are Cl^--selective ligand-gated ion channels that can be assembled from seven subunit classes: $\alpha1$–$\alpha6$, $\beta1$–$\beta3$, $\gamma1$–$\gamma3$, δ, ε, and π, providing the structural basis for extensive heterogeneity of $GABA_A$R structure (Sieghart and Sperk, 2002; Rudolph and Mohler, 2004, 2006). A combination of molecular, biochemical, and genetic approaches suggest that, in the brain, the majority of benzodiazepine receptor subtypes are composed of α, β, and $\gamma2$ subunits (Rudolph and Mohler, 2004). $\gamma2$-containing receptors are highly enriched at synaptic sites in neurons and are responsible for mediating phasic inhibition (Essrich et al., 1998; Kittler and Moss, 2003; Luscher and Keller, 2004).

The number of $GABA_A$Rs on the neuronal cell surface is a critical determinant for the efficacy of synaptic inhibition, and, at steady state, this is determined by the rates of receptor insertion and removal from the plasma membrane. It is evident that $GABA_A$Rs are assembled within the endoplasmic reticulum (ER) and then transported to the plasma membrane for insertion, whereas misfolded or unassembled receptor subunits are rapidly targeted for ER-associated degradation (Gorrie et al., 1997; Kittler and Moss, 2003; Luscher and Keller, 2004). Degradation of ER-retained $GABA_A$Rs is mediated via the activity of the proteasome and is subject to modulation via their association with the ubiquitin-like protein Plic-1 (Bedford et al., 2001). Cell surface $GABA_A$Rs are dynamic entities that exhibit rapid rates of constitutive endocytosis, with internalized receptors being subject to rapid recycling or lysosomal degradation (Kittler and Moss, 2003; Luscher and Keller, 2004; Kittler et al., 2005). Intriguingly, a number of studies have provided evidence that chronic changes in neuronal activity can modulate inhibitory neurotransmission by regulating both presynaptic components in addition to modifying postsynaptic $GABA_A$R levels (Rutherford et al., 1997; Kilman et al., 2002; Hartman et al., 2006). The mechanisms underlying this homeostatic modulation of $GABA_A$R functional expression remain ill defined.

Here we have addressed the role that neuronal activity plays in regulating $GABA_A$R turnover and membrane trafficking and the subsequent accumulation of these proteins on the neuronal plasma membrane. Our results demonstrate that the level of neuronal activity can regulate the ubiquitination of $GABA_A$Rs in the secretory pathway enhancing their degradation primarily within the ER and thereby altering the efficacy of synaptic inhibition. This process decreases the number of receptors inserted into the plasma membrane and their subsequent accumulation at inhib-

Received July 19, 2007; revised Oct. 17, 2007; accepted Oct. 22, 2007.

R.S.S. is supported by a postdoctoral fellowship from the Epilepsy Foundation and G.M. by Deutsche Forschungsgemeinschaft Grant MI 960/1-1 and the Koeln Fortune Program/Faculty of Medicine (University of Cologne). S.J.M. is supported by National Institutes of Health Grants NS046478, NS048045, NS051195, and NS056359, the Medical Research Council (United Kingdom), and the Wellcome Trust. We thank Margie Maronski from the Dichter laboratory for preparation of cultured neurons and Yolande Haydon for manuscript preparation.

Correspondence should be addressed to Dr. Stephen J. Moss at the above address. E-mail: sjmoss@mail.med.upenn.edu.

DOI:10.1523/JNEUROSCI.3277-07.2007

 0270-6474/07/2713341-11$15.00/0

itory synapses. Thus, activity-dependent ubiquitination of $GABA_A$Rs and their subsequent proteasomal degradation may represent a mechanism to regulate the efficacy of synaptic inhibition.

Materials and Methods

Antibodies. Rabbit anti-myc antibody was purchased from Santa Cruz Biotechnology (Santa Cruz, CA). Rabbit polyclonal antibodies against the $GABA_A$R α2, β3, and γ2 subunits have been described previously (Fritschy and Mohler, 1995; Brandon et al., 2000, 2001; Jovanovic et al., 2004), and monoclonal anti-ubiquitin (FK2) was supplied by Biomol (Plymouth Meeting, PA). Synapsin and anti-green fluorescent protein (GFP) were purchased from Synaptic Systems (Goettingen, Germany). Texas Red and cyanine 5 (Cy5)-conjugated secondary antibodies were obtained from Jackson ImmunoResearch (West Grove, PA).

Biotinylation. Neurons or HEK-293 cells grown in 60 mm dishes were chilled on ice for 5 min and then washed twice in PBS with 1 mM $CaCl_2$ and 0.5 mM $MgCl_2$ at 4°C. Cells were incubated for 15 min at 4°C in 1 mg/ml NHS-SS-Biotin (Pierce, Rockford, IL) followed by two 5 min washes in 50 mM glycine to quench unreacted biotin. For the endocytosis assay, neurons were returned to a 37°C incubator for 15 min to allow endocytosis (in the presence of 100 μg/ml leupeptin) and then placed on ice and incubated twice with cleavage buffer (50 mM glutathione, 75 mM NaCl, 10 mM EDTA, 1% bovine serum albumin, and 0.075N NaOH) for 15 min to cleave biotin from cell surface receptors. For the cell surface receptor degradation assay, biotinylated neurons were returned to a 37°C incubator for 24 h in the presence or absence of tetrodotoxin (TTX) (2 μM). After these procedures, neurons were lysed in radioimmunoprecipitation assay (RIPA) buffer: 1% NP-40, 0.5% sodium deoxycholate, 50 mM Tris, pH 8, 150 mM NaCl, and 2 mM EDTA. After correction for protein content using the micro BCA protein assay (Pierce), biotinylated proteins were purified on immobilized avidin (Neutravidin; Pierce) and resolved by SDS-PAGE, and $GABA_A$R levels were measured by immunoblotting with anti-β3 antibody followed by detection with ECL. Blots were imaged in the Fujifilm (Stamford, CT) LAS-3000 imaging system, and band intensities were measured using Fujifilm Multi Gauge software.

Cell culture and transfection. HEK-293 cells were transfected using electroporation with 10 μg of DNA as outlined previously (Taylor et al., 1999, 2000). Cortical and hippocampal neurons were obtained from embryonic day 18 (E18) rats (Kittler et al., 2000; Jovanovic et al., 2004). Dissociated E18 rat neurons were transfected with 3 μg of plasmid DNA per 5×10^6 neurons using the Rat Nucleofector kit (Amaxa, Gaithersburg, MD) (Couve et al., 2004; Kittler et al., 2004; Jacob et al., 2005). For pulse-chase analysis, cortical neurons were incubated in methionine free medium (DMEM) for 20 min and then labeled with 500 mCi/ml [^{35}S]methionine (PerkinElmer, Waltham, MA) for 30–40 min. Neurons were then washed and incubated in complete neurobasal media with an excess of cold methionine (100×) for an additional 0–8 h.

Electrophysiology. Membrane currents from HEK-293 cells were measured as outlined previously (Taylor et al., 1999, 2000; Bedford et al., 2001; Kittler et al., 2004, 2005; Jacob et al., 2005). Miniature IPSCs (mIPSCs) were recorded from 14–21 d *in vitro* (DIV) cultured hippocampal neurons in the whole-cell voltage-clamp configuration (−70 mV) as detailed previously (Kittler et al., 2004, 2005). Briefly, all experiments were performed at room temperature (22–23°C). Extracellular bath solution was composed of the following (in mM): 140 NaCl, 4.7 KCl, 10 HEPES, 11 glucose, 1.2 $MgCl_2$, and 2.5 $CaCl_2$, adjusted to pH 7.4 with NaOH. Borosilicate pipettes (3–6 MΩ) were filled with the following (in mM): 150 CsCl, 10 HEPES, 1.1 EGTA, 2 $MgCl_2$, 0.1 $CaCl_2$, and 1 Mg^{2+}-ATP, adjusted to pH 7.2 with CsOH. Recordings were started 5–10 min after a stable whole-cell access was obtained. mIPSCs were recorded in the presence of 200 nM tetrodotoxin (Sigma-Aldrich, St. Louis, MO), 10 μM 6-cyano-7-nitroquinoxaline-2,3-dione (Sigma-Aldrich), and 20 μM 2-D-aminophosphonopentanoic acid (Sigma-Aldrich). An Axopatch 200B amplifier and Digidata 1322A (Molecular Devices, Sunnyvale, CA) software were used for pulse generation, data acquisition (10 kHz), and filtering (5 kHz, four-pole Bessel filter). Synaptic currents were recorded using an Axopatch 200B amplifier (Molecular Devices), filtered at 2 kHz, sampled at 5 kHz, digitized (Digidata 1320A; Molecular Devices), and stored for off-line analysis [using Minianalysis (Synaptosoft, Decatur GA) and IGOR Pro (WaveMetrics, Lake Oswego, OR)]. Access resistance (10–18 MΩ; 80% compensation) was monitored using a −5 mV voltage, applied every 120 s, and data from cells were discarded when >15% change occurred. Miniature events were analyzed using pClamp 9.2 (Clampfit; Molecular Devices) and MiniAnalysis 6.0.3 software (Synaptosoft, Leonia, NJ) using pooled population data from expressed as mean ± SEM. An individual event was defined as being >2.5 SDs from the average background noise. The decay phase was fitted with a monoexponential function (τ decay). Rise time was also analyzed by comparing the mean 10–90% rise time.

Immunofluorescence. Transfected neurons were fixed in 4% paraformaldehyde, stained without membrane permeabilization with rabbit anti-GFP, and then permeabilized with 0.1% Triton X-100 for 4 min. They were then labeled with anti-synapsin antibodies, visualized by confocal microscopy (blind to experimental condition), and analyzed using MetaMorph (Molecular Devices) software. Receptor clusters were defined as being ~0.5–2 μm in length and approximately twofold to threefold more intense than background diffuse fluorescence and were colocalized with or directly apposed to synapsin staining. Clusters farther than 1 μm from presynaptic marker staining were considered extrasynaptic. To quantify the number of synapses, thresholds were set and kept constant for control and test neurons. To measure the role of ubiquitination in regulating $GABA_A$R membrane insertion, we used β3 and $\beta3^{K12R}$ expression constructs modified at the N terminus with a pHluorin reporter and the minimal α-bungarotoxin (Bgt) binding site peptide (BBS). These are termed $^{BBS}\beta$3 and $^{BBS}\beta3^{K12R}$, respectively (Scherf et al., 2001; Katchalski-Katzir et al., 2003; Sekine-Aizawa and Huganir, 2004; Bogdanov et al., 2006). $^{BBS}\beta$3 synaptic puncta were counted from 1-bit binary masks. Data were analyzed from 15–20 neurons for each condition (50 μm per dendrite per cell). To quantify fluorescence intensity of $^{BBS}\beta$3 synaptic staining, images of neurons were thresholded to a point at which dendrites were outlined. Synapsin staining was thresholded to a set value and kept constant for control and test neurons. Next a 50 μm section along a given proximal dendrite was selected, and a 1-bit binary image (exclusive) was made of the synapsin staining in the outlined dendrite. We then subtracted away all $^{BBS}\beta$3 staining that did not colocalize with the binarized synapsin staining. As a result, only $^{BBS}\beta$3 staining that colocalized with synapsin remained, and the average fluorescence intensity of these $^{BBS}\beta$3puncta was determined. Data were analyzed from 15–20 neurons for each condition from at least two to three different cultures. Finally, puncta selection and analysis were all performed blind to experimental condition.

Immunoprecipitation. HEK-293 cells or neurons were lysed in 1% SDS, 25 mM Tris, pH 7.4. Lysates were diluted 10-fold with RIPA buffer lacking SDS: 50 mM Tris, pH 8, 150 mM NaCl, 1% NP-40, 0.5% sodium deoxycholate, 2 mM EDTA plus 1 μM ubiquitin aldehyde (Biomol), and mammalian protease inhibitor cocktail (Sigma-Aldrich). After correction for protein content, lysates were immunoprecipitated with rabbit anti-myc IgGs (Santa Cruz Biotechnology) or anti-β3 antibodies as detailed previously (Brandon et al., 2000, 2001; Jovanovic et al., 2004; Kittler et al., 2004). Precipitated material was then subject to SDS-PAGE and immunoblotting.

Membrane insertion assays. HEK-293 cells expressing $GABA_A$R α1 and $^{BBS}\beta$3 subunits were incubated with 10 μg/ml unlabeled α-Bgt for 20 min at 4°C (to inhibit endocytosis), washed in PBS, and incubated with 10 μg/ml biotin-conjugated Bgt at 37°C for up to 20 min to label newly inserted receptors. After lysis, biotin–Bgt/$^{BBS}\beta$3 complexes were purified on neutravidin and immunoblotted with anti-β3 antibodies. To measure insertion in neurons nucleofected 15 DIV hippocampal cultures were labeled at 37°C with 10 μg/ml rhodamine (Rd)-conjugated Bgt for 15 min, washed, and incubated for an additional 5 min with 10 μg/ml Alexa-Fluor-647 (Alx)-conjugated Bgt. All incubations were performed in the presence of 5 μM tubocurarine (Sigma-Aldrich) to block Bgt binding to endogenous acetylcholine receptors (Sekine-Aizawa and Huganir, 2004; Bogdanov et al., 2006). All Bgt derivatives were obtained from Invitrogen (Carlsbad, CA). Cells were fixed in 4% paraformaldehyde, and confocal images were collected using a 60× objective lens acquired

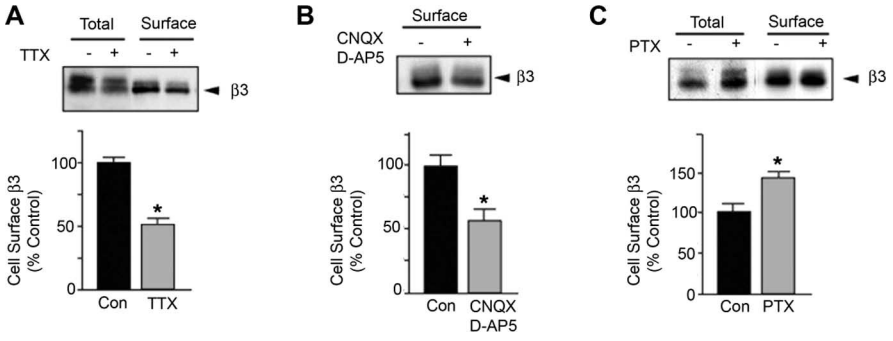

Figure 1. Neuronal activity regulates the cell surface stability of $GABA_A$Rs. ***A***, Chronic blockade of neuronal activity reduces $GABA_A$Rs expression. Cortical neurons (>16 DIV) were incubated with or without 2 μM TTX for 24 h and then subject to biotinylation with NHS-SS-Biotin. Equal amounts of detergent-soluble protein were added to immobilized avidin and then immunoblotted with anti-β3 antibody. The cell surface levels of $GABA_A$Rs incorporating β3 subunits were measured in control (Con) and assigned a value of 100%. *$p < 0.05$, significantly different from control (*t* test; $n = 5$). Error bars indicate ± SEM. ***B***, Glutamate receptor antagonists decrease cell surface levels of $GABA_A$Rs. Cortical neurons at 16 DIV were incubated with or without the AMPA receptor antagonist CNQX (10 μM) and the NMDA receptor antagonist D-AP-5 (20 μM). *$p < 0.05$, significantly different from control (*t* test; $n = 5$). Error bars indicate ± SEM. ***C***, $GABA_A$R antagonist increase $GABA_A$R cell surface expression levels. Cortical neurons at 16 DIV were treated with 20 μM PTX for 24 h, and cell surface β3 subunit levels were measured via biotinylation as detailed above. The cell surface levels of $GABA_A$Rs incorporating β3 subunits were measured in control and assigned a value of 100%. *$p < 0.05$, significantly different from control (*t* test; $n = 6$). Error bars indicate ± SEM.

with Olympus Optical (Tokyo, Japan) Fluoview version 1.5 software, and the same image acquisition settings for $^{BBS}\beta3$ and $^{BBS}\beta3^{K12R}$ (Bogdanov et al., 2006) were used. These images were analyzed using MetaMorph imaging software (Universal Imaging, Downingtown, PA). First, a three-dimensional reconstruction of an imaged neuron was made from a series of Z sections, and then the average fluorescence intensity of Alexa-Fluor-647–Bgt staining per 250 μm of dendrite was measured from three dendrites per neuron, after subtraction of background fluorescence.

Mutagenesis. Site-directed mutagenesis of the β3 subunit was performed using the QuickChange mutagenesis kit (Stratagene, La Jolla, CA).

Statistical analysis. Statistical significance was assessed using either Student's paired *t* test or the Kolmogorov–Smirnov two-sample test, in which $p < 0.05$ was considered significant.

Results

Chronic changes in neuronal activity regulate the numbers of $GABA_A$R expressed on the neuronal cell surface

To commence our studies, we used cultured cortical neurons that had been maintained for at least 14 d DIV and have been demonstrated to exhibit hyperpolarizing $GABA_A$R responses (Woodin et al., 2003; Fiumelli et al., 2005). The effects of the voltage-gated Na^+ channel blocker TTX on the number of cell surface $GABA_A$Rs containing β3 subunits was then examined. After cell lysis and correction for protein content, biotinylated proteins were purified on avidin and immunoblotted with antibodies specific to the β3 subunit (Jovanovic et al., 2004; Kittler et al., 2004). We chose to study primarily $GABA_A$R subtypes containing β3 subunits because gene knock-out has revealed that these proteins are critical for neuronal function and animal survival (Homanics et al., 1997). Treatment of cultures with 2 μM TTX for 24 h resulted in a significant decrease (to 47.8 ± 5.3% of control) (Fig. 1*A*) in cell surface levels of $GABA_A$Rs containing β3 subunits. The total expression of receptor β3 subunits was also reduced by this treatment (to 45 ± 6.7% of control) (Fig. 1*A*). Similar statistically significant decreases in the cell surface expression levels of $GABA_A$R α2 and γ2 subunits were also evident (supplemental Fig. 1, available at www.jneurosci.org as supplemental material), suggesting that chronic neuronal inactivity leads to the loss of functional heteromeric cell surface $GABA_A$Rs. In addition TTX treatment also significantly decreased the number of cell surface $GABA_A$Rs containing β3 subunits in 16 DIV hippocampal neurons (supplemental Fig. 2, available at www.jneurosci.org as supplemental material).

To corroborate our experiments with TTX, we assessed the effects of blocking excitatory synaptic transmission on the cell surface levels of $GABA_A$Rs with glutamate receptor antagonists, which have been established to reduce neuronal activity in culture (Rao and Craig, 1997; O'Brien et al., 1998). Blockade of glutamate receptors significantly decreased the cell surface expression levels of $GABA_A$Rs containing β3 subunits to 45.8 ± 13.1% of control (Fig. 1*B*). We also examined the effects of chronically increasing neuronal activity on the cell surface expression levels of $GABA_A$Rs using picrotoxin (PTX) (40 μM), a $GABA_A$R antagonist and has been shown to increase the activity of neuronal cultures (Rao and Craig, 1997; O'Brien et al., 1998). In contrast to the effects of TTX and glutamate receptor antagonists, treatment of neurons with PTX significantly increased both the cell surface (by 55 ± 2.3% of control) and total (by 47 ± 8.5% of control) expression levels of the $GABA_A$Rs β3 subunit (Fig. 1*C*).

To assess whether the reduced levels of cell surface $GABA_A$Rs evident with TTX alters synaptic inhibition we compared the properties of mIPSCs in hippocampal neurons (>16 DIV) treated with or without TTX. mIPSCs were isolated by adding the excitatory amino acid antagonists (10 μM CNQX, 20 μM D-AP-5) and TTX (2 μM) to the bath solution as described previously (Kittler et al., 2004, 2005; Chen et al., 2006). Under these conditions remaining events were blocked by picrotoxin (20 μM) indicating that these events were dependent upon the activation of $GABA_A$Rs (data not shown). As illustrated in Figure 2*A–D*, TTX-treated neurons exhibited a significant shift in peak amplitude and frequency compared with controls. Quantifying these observations, the mean amplitude of mIPSCs in TTX-treated neurons was 41.8 ± 3.3 pA ($n = 9$), significantly lower (Fig. 2*E*) ($p < 0.05$) than the value of 50.7 ± 1.9 pA ($n = 8$) evident in control neurons. In addition, the average frequency of mIPSCs in TTX-treated neurons was 0.5 ± 0.1 Hz ($n = 14$), significantly lower (Fig. 2*E*) ($p < 0.05$) than values evident in controls (0.9 ± 0.1 Hz; $n = 14$). However, the 10–90% rise time and decay time constants were unaltered in neurons treated with TTX compared with control (Fig. 2) (supplemental Fig. 3, available at www.jneurosci.org as supplemental material). Although alterations in mIPSC amplitude may reflect modified transmitter release or altered channel kinetics, they are also indicative of altered numbers of synaptic receptors. Consistent with decreased mIPSC amplitude, deficits in the number of cell surface β3 subunits are also evident in cortical hippocampal neurons treated with TTX as measured via biotinylation (Fig. 1) (supplemental Fig. 2, available at www.jneurosci.org as supplemental material), suggesting that the cell surface expression levels of $GABA_A$Rs are subject to regulation by the level of neuronal activity.

Chronic changes in neuronal activity regulate the levels of $GABA_A$R β3-subunit ubiquitination

To further examine the role that activity plays in regulating $GABA_A$R expression levels, we tested the effects of TTX on sub-

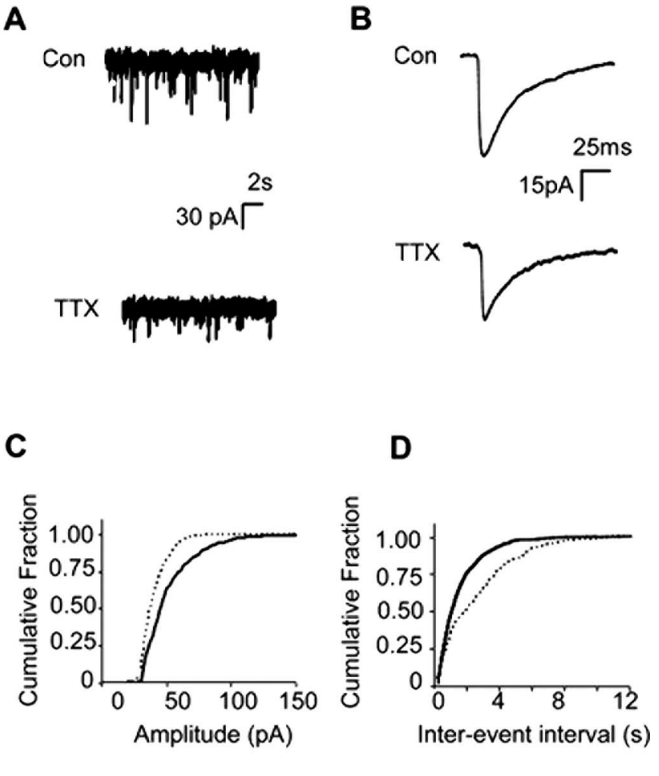

E

Parameter	Control	TTX
Peak amplitude (pA)	50.7 ± 1.95	41.8 ± 3.32*
10-90 % rise time (ms)	2.43 ± 0.32	2.20 ± 0.34
τ decay (ms)	39.1 ± 1.64	36.7 ± 1.79
Frequency (Hz)	0.98 ± 0.16	0.50 ± 0.11*

Figure 2. TTX treatment modulates the properties of mIPSCs. ***A–E***, The properties of mIPSCs were compared in control (Con) neurons or those treated with TTX for 18–24 h. Representative sweeps showing mIPSCs recorded from control and TTX-treated neurons are shown in ***A***, whereas representative typical mIPSC events for control and TTX-treated hippocampal neurons are illustrated in ***B***. Cumulative probability data for mIPSC amplitude and interval events are shown in ***C*** and ***D***, respectively, with the dashed lines representing TTX-treated neurons and the solid lines representing controls. Data were pooled with an equal number of amplitudes and intervals being used for each condition (2000 events per cell). The parameters of mIPSC in control neurons and those treated with TTX are shown in ***E***. Amplitude and frequency is presented as mean ± SEM. *$p < 0.05$, significantly different from control (Kolmogorov–Smirnov test; $n = 8–9$). Decay and rise times were determined from the data shown in supplemental Figure 3 (available at www.jneurosci.org as supplemental material).

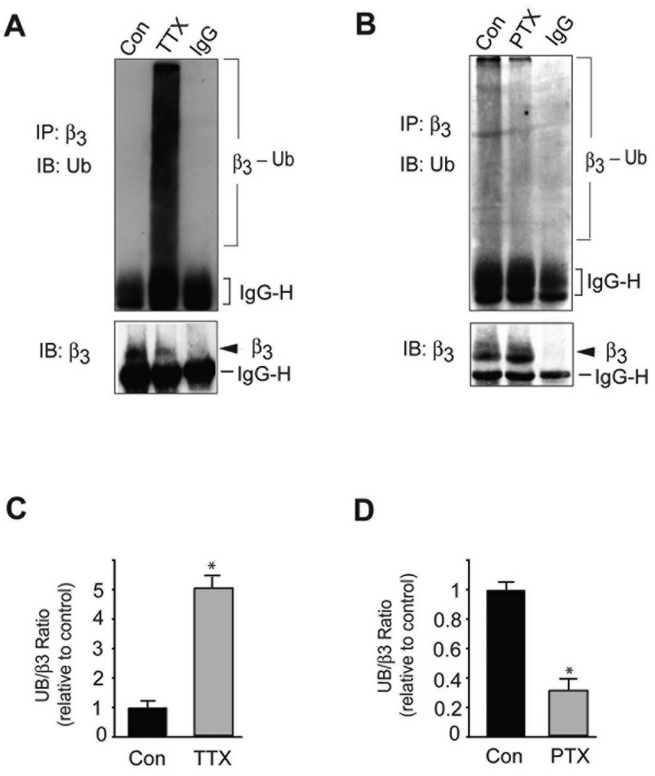

Figure 3. Activity-dependent ubiquitination of the $GABA_AR$ β3 subunit. ***A***, Chronic blockade of neuronal activity increases the levels of $GABA_AR$ β3 ubiquitin (Ub) conjugates. Cortical neurons (16 DIV) were treated with or without TTX (2 μM) for 24 h. The β3 subunit was immunoprecipitated (IP) under denaturing conditions with anti-β3 antibody or control non-immune IgGs from equal amounts of solubilized protein. Precipitated β3 was subject to immunoblotting (IB) with anti-polyubiquitin (FK2), and then the blots were stripped and reprobed with anti-β3 IgGs as indicated. ***B***, Chronically increasing neuronal activity with PTX decreases the levels of β3 ubiquitin conjugates. Cortical neurons (16 DIV) were treated with or without 50 μM PTX for 24 h. The β3 subunit was immunoprecipitated and immunoblotted with FK2 and anti-β3 IgGs as outlined in ***A***. ***C***, ***D***, The ubiquitin/β3 subunit ratios were calculated from neurons exposed to TTX, PTX, or control (Con) neurons as indicated, and the data in control were given a value of 1. *$p < 0.05$, significantly different from control (*t* test; $n = 3$). Error bars represent ± SEM.

unit ubiquitination. To do so, we immunoprecipitated β3 subunits under denaturing conditions and immunoblotted precipitated material with an antibody that recognizes polyubiquitin (FK2). Typical of protein ubiquitination (Haglund et al., 2003b; Haglund and Dikic, 2005), a smear of immunoreactivity between 66 and 250 kDa was seen with FK2 antibody immunoprecipitating with anti-β3 but not control IgG (Fig. 3*A*,*B*). This reaction product represents the addition of multiple 7.6 kDa ubiquitin moieties to various (>20) lysine residues within the $GABA_AR$ β3 subunit. By measuring the intensity of the FK2 reaction product between 66 and 250 kDa, it was evident that activity blockade with TTX produced a large (5.0 ± 0.5-fold) increase in the levels of β3 subunit ubiquitination (Fig. 3*A*,*C*) and decreased total cellular levels of the β3 subunit. In contrast, treatment of neurons with PTX induced a substantial (3.1 ± 0.3-fold) decrease in the levels of ubiquitinated β3 and increased total cellular levels of this receptor subunit (Fig. 3*B*,*D*).

Polyubiquitination of proteins enhances their targeting to and degradation by the proteasome (Glickman and Ciechanover, 2002); thus, we analyzed the role that blocking proteasome activity with epoxomicin (EP) (20 μM) has on activity-dependent turnover of $GABA_ARs$. EP blocked the effects of TTX on cell surface expression levels of $GABA_ARs$ receptors and also significantly increased their cell surface expression levels compared with control (117.5 ± 2.8%) (Fig. 4*A*). Moreover, EP enhanced the level of β3 subunit ubiquitination to 250.4 ± 20.8% of control (and significantly increased the cell surface levels of β3-containing $GABA_ARs$ by 159.3 ± 8.1% of control levels (Fig. 4*B–D*).

Cell surface $GABA_ARs$ undergo constitutive endocytosis and are eventually targeted for degradation principally in the lysosome (Kittler et al., 2000, 2004). We thus asked whether chronic activity blockade had any influence on the degradation of cell surface $GABA_ARs$, which reflects their levels of endocytosis, endocytic sorting, and lysozomal degradation. Using biotinylation, it was evident that TTX did not significantly alter the degradation of surface β3 subunits (Fig. 4*E*), suggesting that neuronal activity acts principally to regulate $GABA_AR$ stability and/or insertion in the secretory pathway.

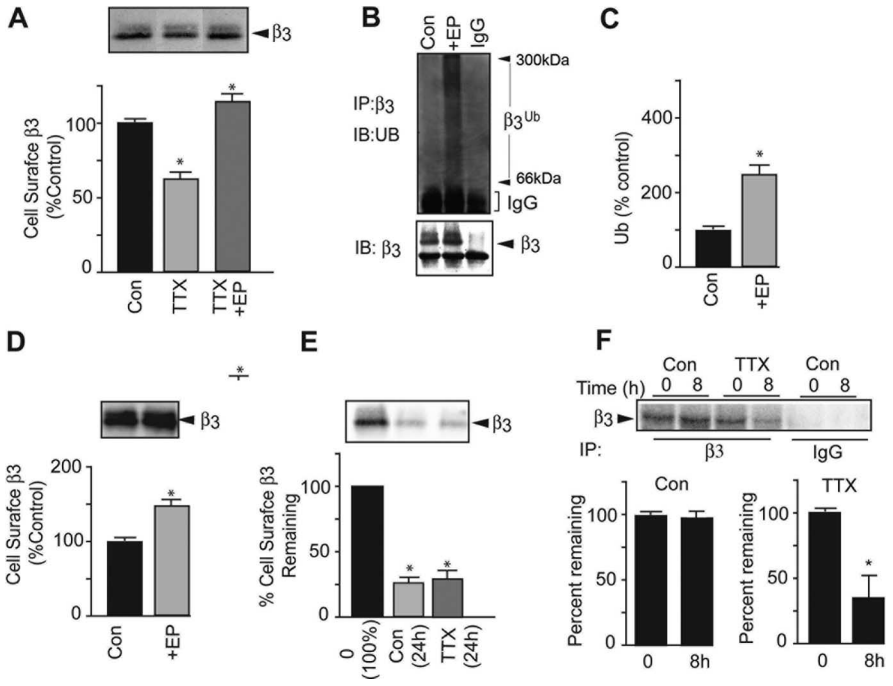

Figure 4. Regulation of GABA$_A$R cell surface expression by activity blockade is dependent on proteasome activity. ***A***, Proteasome inhibition blocks the effects of TTX on GABA$_A$R cell surface expression. Cortical neurons (16 DIV) were treated with or without TTX for 24 h, and 20 μM EP was added for the last 8 h of the TTX incubation as indicated. Neurons were then labeled with NHS-SS-Biotin and lysed. Biotinylated proteins were isolated with immobilized avidin and then immunoblotted with anti-β3 IgGs. The levels of β3 subunit cell surface expression were then determined, and those in control (Con) cultures were given a value of 100%. *$p < 0.05$, significantly different from control (*t* test; $n = 3$). Error bars indicate ± SEM. ***B***, EP stabilized GABA$_A$R β3 ubiquitin (Ub) conjugates. Cortical neurons (16 DIV) were treated with or without 20 μM EP for 8 h. The β3 subunit was immunoprecipitated (IP) with anti-β3 IgGs or control non-immune IgGs from equal amounts of solubilized protein. Precipitated β3 was subject to immunoblotting (IB) with anti-polyubiquitin (FK2), and then blots were stripped and reprobed with anti-β3 IgGs as indicated. ***C***, Quantification of the increase in β3 ubiquitin conjugates after epoxomicin treatment. The ubiquitin signal was expressed as an *x*-fold increase relative to control. *$p < 0.05$, significantly different from control (*t* test; $n = 3$). Error bars represent ± SEM. ***D***, Proteasome inhibition increase the level of GABA$_A$Rs expressed at the cell surface. Cortical neurons (16 DIV) were incubated with or without 20 μM EP for 8 h. Cell surface proteins were labeled with NHS-SS-Biotin, isolated with avidin, and immunoblotted with anti-β3 IgGs. *$p < 0.05$, significantly different from control (*t* test; $n = 3$). Error bars represent ± SEM. ***E***, Activity blockade does not regulate the degradation of GABA$_A$Rs existing at the cell surface. Cortical neurons (16 DIV) were biotinylated and then incubated at 37°C for 24 h with or without TTX as indicated, whereas neurons at time 0 were lysed and snap frozen. Biotinylated receptors were isolated as in ***A***. β3 subunit band intensities were measured, and the levels at time 0 were assigned a value of 100% ($n = 3$; error bars represent ± SEM). ***F***, Chronic inactivity increases the turnover of GABA$_A$Rs. Neurons at 16–18 DIV were treated with TTX for 24 h, followed by a pulse chase with [^{35}S]methionine. Cultures were lysed and immunoprecipitated with anti-β3 antibodies or control IgG under denaturing conditions and subject to SDS-PAGE as shown in the top. Band intensities were quantified using a phosphorimager. Data were then normalized to the levels at time 0, which were assigned a value of 100%. *$p < 0.05$, significantly different from control at 8 h (*t* test; $n = 3$). Error bars represent ± SEM.

To further test this, we used pulse-chase analysis with [^{35}S]methionine after a 24 h incubation period with TTX. This revealed that 89.9 ± 3.5% of newly synthesized β3 subunits were still present after the chase period. However, in the presence of TTX, this value was decreased to 35.8 ± 12.4% of that present at time 0 (Fig. 4*F*). To determine whether the observed increased rate of degradation of the β3 in the presence of TTX results from increased ER-associated degradation, we performed a pulse-chase experiment in the presence of Brefeldin A, an established inhibitor of ER-Golgi transport. Even in the presence of Brefeldin A, turnover of the β3 subunit was increased in TTX-treated neurons (supplemental Fig. 4, available at www.jneurosci.org as supplemental material). Because GABA$_A$R assembly takes place principally in the ER (Connolly et al., 1996; Gorrie et al., 1997), this decreased stability of newly synthesized receptors in the presence of TTX and Brefeldin A suggest that chronic inactivity acts to principally control receptor stability in the ER.

Identification of major sites for ubiquitination within the GABA$_A$R β3 subunit

To further examine the role of ubiquitination in regulating GABA$_A$R trafficking, we used mutagenesis to convert all 12 candidate lysine residues for ubiquitination within the major intracellular loop of the β3 subunit to arginines in addition to adding the myc epitope at the N terminus of this protein ($^{M}\beta3^{K12R}$) (supplemental Fig. 5, available at www.jneurosci.org as supplemental material) (Taylor et al., 2000). $^{M}\beta3^{K12R}$ exhibited a large decrease (to 55.4 ± 5.4% of control) (Fig. 5*A*) in ubiquitination compared with $^{M}\beta3$, demonstrating that major sites for this covalent modification reside within the intracellular domain of this GABA$_A$R subunit. Other sites for ubiquitination presumably reside within the transmembrane or extracellular domains of the β3 subunit that would be subject to ubiquitination preceding proteasomal degradation (Haglund et al., 2003a). Consistent with the reduced level of ubiquitination, we observed a significant increase (to 145 ± 4.5% of control) (Fig. 5*B*) in the cell surface expression levels of $^{M}\beta3^{K12R}$ compared with $^{M}\beta3$.

To control for possible deleterious effects of the mutations on GABA$_A$R functional expression, we assessed the ability of the $^{M}\beta3^{K12R}$ subunit to assemble with receptor α1 and γ2 subunits using patch-clamp recording in HEK-293 cells (Taylor et al., 2000; Jacob et al., 2005; Bogdanov et al., 2006). We first assessed the sensitivity of the expressed receptors to benzodiazepine modulation, a property critically dependent on the production of heteromeric $\alpha1\beta3\gamma2$ receptors (Sieghart and Sperk, 2002; Mohler et al., 2005). Flurazepam (100 nM) produced similar robust enhancements of I_{GABA} of ~200% for receptors composed of $\alpha1\beta3\gamma2$ or $\alpha1\beta3^{K12R}\gamma2$ subunits (Fig. 5*C*). Equilibrium GABA concentration–response curves for receptors incorporating $^{M}\beta3^{K12R}$ or $^{M}\beta3$ subunits yielded similar EC_{50} values of 9.40 ± 1.80 and 10.17 ± 2.42 μM, respectively, values that were not significantly altered by preincubation with the proteasome inhibitor MG132 [carbobenzoxy-L-leucyl-L-leucyl-L-leucinal] (Fig. 5*D*). We also examined the effects of MG132 on the maximal currents. For receptors incorporating $^{M}\beta3$, there was a large and highly significant increase in the magnitude of I_{GABA} using saturating agonist concentrations, an effect that was not replicated for those incorporating $^{M}\beta3^{K12R}$ subunits (Fig. 5*E*).

Together, our results demonstrate that major sites for ubiquitination reside within the intracellular domain of the GABA$_A$R β3 subunit and that mutation of these residues leads to increased receptor functional expression. They also suggest that these lysine residues within the intracellular domain of the β3 subunit play a role in ubiquitin-dependent proteasomal degradation of this subunit.

Decreasing β3 subunit ubiquitination increases receptor accumulation on the neuronal cell surface

To examine the relevance of our recombinant studies for $GABA_A$Rs in their native environment, we expressed $^{M}\beta3$ and $^{M}\beta3^{K12R}$ subunits in cultured cortical neurons using nucleofection. After immunoprecipitation with rabbit anti-myc antibodies and blotting with FK2 antibody, it was evident that ubiquitination of $^{M}\beta3^{K12R}$ was decreased to 50.1 ± 4.5% of control (Fig. 6*A*). Consistent with this, the cell surface expression levels of $GABA_A$Rs incorporating $^{M}\beta3^{K12R}$ subunits were higher than those incorporating $^{M}\beta3$ subunits (by 141.2 ± 8.2% of control) (Fig. 6*B*). A concern in these experiments is that there is a possible formation of β3 homomeric receptors, but it should be noted that this phenomenon was only observed when β3 was expressed alone in HEK-293 cells or oocytes (Taylor et al., 1999). This unique property of β3 subunit homomerization is totally suppressed on coexpression with $GABA_A$R α and/or γ2 subunits. It should also be noted that β3 homomers are very unstable with a half-life of 2 h (Wooltorton et al., 1997; Taylor et al., 1999). Given that neurons express high levels of endogenous $GABA_A$R α and γ subunits, the presence of β3 homomers is unlikely to be a factor in our experiments.

In principle, the elevated accumulation of receptors incorporating $\beta3^{K12R}$ on the plasma membrane may reflect changes in either endocytic sorting and/or lysosomal degradation, or in higher rates of insertion from the secretory pathway. Using biotinylation, it was evident that receptors containing $^{M}\beta3$ and $^{M}\beta3^{K12R}$ exhibited very similar levels of endocytosis over a 15 min time course (21.3 ± 4.2 vs 20.9 ± 6.2%, respectively) (Fig. 6*C*), comparable with levels seen for the endogenous β3 subunit (Kittler et al., 2004). Moreover, cell surface $GABA_A$Rs containing $^{M}\beta3$ and $^{M}\beta3^{K12R}$ exhibited very similar rates of degradation over 10 h of 33.5 ± 3.2 and 34.6 ± 3.6%, respectively (Fig. 6*D*). Together, these results suggest that ubiquitination of the β3 subunit does not primarily act to regulate the endocytic sorting/lysosomal degradation of $GABA_A$Rs but may act to modulate their insertion, from the secretory pathway, into the plasma membrane.

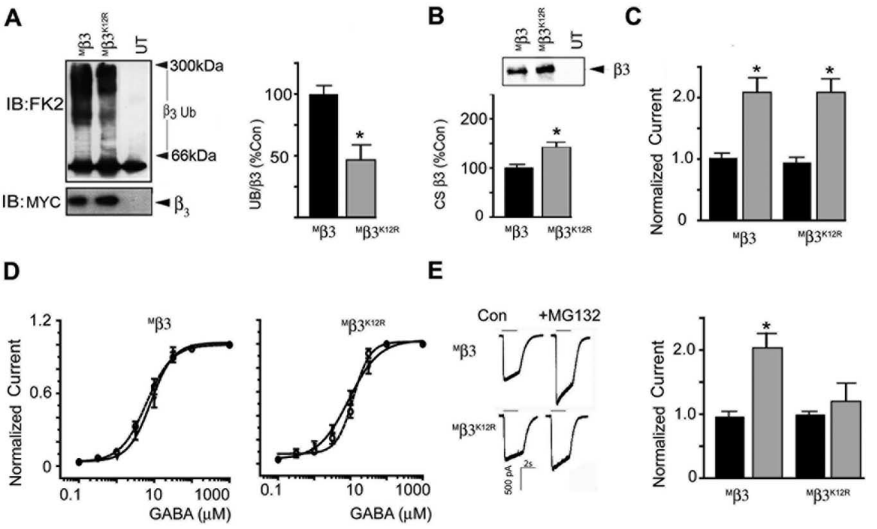

Figure 5. Analyzing the properties of heteromeric $GABA_A$Rs incorporating $\beta3^{K12R}$ subunits. ***A***, $\beta3^{K12R}$ subunits exhibit decreased levels of ubiquitination (Ub). HEK-293 cells expressing $GABA_A$R $^{M}\beta3$ or $^{M}\beta3^{K12R}$ subunits, modified with an N-terminal myc tag (M), or untransfected control cells (UT) were lysed in 1% SDS and diluted 10-fold. $^{M}\beta3$ and $^{M}\beta3^{K12R}$ subunits were immunoprecipitated (IP) with rabbit anti-myc IgGs, and precipitated material was immunoblotted (IB) with monoclonal anti-polyubiquitin (FK2) or anti-myc IgGs as indicated. The UB/$^{M}\beta3$ and UB/$^{M}\beta3^{K12R}$ ratios were calculated and normalized to UB/$^{M}\beta3$. $^{*}p < 0.05$, significantly different from control (UB/$^{M}\beta3$) (*t* test, $n = 3$). Error bars represent ± SEM. ***B***, Enhanced cell surface expression levels of $GABA_A$Rs incorporating $^{M}\beta3^{K12R}$ subunits. HEK-293 cells expressing receptor $^{M}\beta3$ or $^{M}\beta3^{K12R}$ subunits and untransfected controls (UT) were labeled with NHS-SS-Biotin and lysed. Equal amounts of solubilized protein were added to immobilized avidin to isolate biotinylated receptors, which were then subject to immunoblotting with anti-myc IgGs. Cell surface levels were measured, and values were normalized to $^{M}\beta3$ levels ($^{*}p < 0.05$, significantly different from $^{M}\beta3$, *t* test; $n = 3$). ***C***, Benzodiazepine modulation of $\alpha1^{M}\beta3\gamma2$ and $\alpha1^{M}\beta3^{K12R}\gamma2$ receptors. HEK-293 cells expressing $GABA_A$Rs were voltage clamped at −70 mV. The magnitude of I_{GABA} at 2 μM GABA agonist concentration was then measured in the absence (black bars) and presence (gray bars) of 100 nM flurazepam. Normalized conductances in the absence of 100 nM flurazepam were given a value of 1. $^{*}p < 0.05$, significantly different from control (unpaired *t* test; $n = 7$–9 cells). Error bars represent ± SEM. ***D***, Inhibiting the proteasome does not alter agonist sensitivity of $GABA_A$Rs. Equilibrium GABA concentration–response curves obtained from HEK-293 cells expressing $GABA_A$Rs composed of $\alpha1^{M}\beta3$ and $\alpha1^{M}\beta3^{K12R}$ subunits, respectively, in the presence and absence of 20 min pretreatment with 20 μM MG132. In each cell, the GABA-activated current was normalized to the conductance evoked by 1000 μM GABA. Each point represents the mean ± SEM ($n = 6$–8). HEK-293 cells were voltage clamped at −50 mV holding potential. The curves were generated by the equation $g = g_{max}(1/1 + EC_{50}/[A]^{n})$, where g and g_{max} represent the conductance induced by a concentration, A, and saturating concentration of GABA, respectively. EC_{50} represents the GABA concentration required to evoke half-maximal response, and n_H is the Hill slope. ***E***, Inhibiting the activity of the proteasome enhances the maximal current for $GABA_A$Rs containing wild-type β3 subunits. HEK-293 cells expressing $GABA_A$Rs composed of $\alpha1^{M}\beta3$ ($^{M}\beta3$) and $\alpha1^{M}\beta3^{K12R}$ ($^{M}\beta3^{K12R}$) subunits were exposed to 20 μM MG132 for 20 min, and the magnitude of the conductances induced by 1000 μM GABA was compared with those in control cells (Con) and those exposed to MG132 (+MG132). Typical traces are shown in the left. Data were normalized to the conductances seen in control, which were assigned a value of 100%. $^{*}p < 0.05$, significantly different from control (*t* test; $n = 7$–9 cells). Error bars represent ± SEM.

Ubiquitination of the β3 subunit modulates $GABA_A$R insertion into the plasma membrane

To measure the role of ubiquitination in regulating $GABA_A$R membrane insertion, we used β3 and $\beta3^{K12R}$ expression constructs modified at the N terminus with a pHluorin reporter and the minimal BBS. These are termed $^{BBS}\beta3$ and $^{BBS}\beta3^{K12R}$, respectively (Scherf et al., 2001; Katchalski-Katzir et al., 2003; Sekine-Aizawa and Huganir, 2004; Bogdanov et al., 2006). We previously established that the addition of these reporters to $GABA_A$Rs is functionally silent but allows the selective visualization of cell surface receptor populations in both expression systems and cultured neurons (Jacob et al., 2005; Bogdanov et al., 2006). These engineered receptors also bind Bgt with high affinity (7.2×10^{-9} M) with an off-rate in excess of 5 h, facilitating the analysis of $GABA_A$R insertion in living neurons (Bogdanov et al., 2006).

We initially characterized the insertion rate of $GABA_A$Rs composed of $\alpha1^{BBS}\beta3$ in HEK-293 cells by first labeling existing cell surface populations with 10 μg/ml Bgt. After extensive washing, cells were labeled with 10 μg/ml biotinylated Bgt for varying time periods at 37°C before lysis. Bgt/$GABA_A$R complexes were then isolated with immobilized avidin and immunoblotted with anti-GFP antibodies. A band of ~89 kDa representing the $^{BBS}\beta3$ subunit was evident after 2.5 min incubation at 37°C but not at the time 0 point (Fig. 7*A*). This band was not detected in untransfected cells (Fig. 7*A*). Its appearance could be blocked by coincubation with 10 μg/ml unlabeled Bgt (data not shown). $GABA_A$R insertion appeared to be linear during the first 5 min of incubation before saturating after 20 min (Fig. 7*A*). We therefore used a time point of 2.5 min to compare membrane insertion for $^{BBS}\beta3$

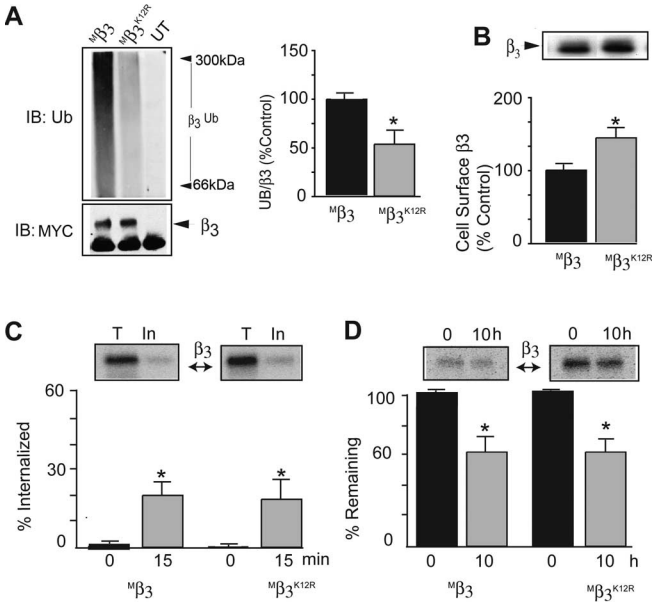

Figure 6. Decreased ubiquitination and enhanced cell surface accumulation of GABA$_A$Rs incorporating $^{M}\beta3^{K12R}$ in neurons. ***A***, Decreased ubiquitination (Ub) of GABA$_A$R $^{M}\beta3^{K12R}$ subunits in cortical neurons. Nucleofected neurons (5 DIV) were lysed in 1% SDS and diluted 10-fold. $^{M}\beta3$ and $^{M}\beta3^{K12R}$ subunits were immunoprecipitated (IP) with rabbit anti-myc IgGs, and precipitated material was immunoblotted (IB) with monoclonal anti-ubiquitin (FK2). Blots were then stripped and reprobed with anti-myc IgGs, as indicated. The ratio of UB/$\beta3$ signals was then determined, and values for UB/$^{M}\beta3$ (control) were assigned a value of 100%. $^{*}p < 0.05$, significantly different from control (*t* test; $n = 4$). ***B***, Enhanced cell surface accumulation of GABA$_A$Rs containing $^{M}\beta3^{K12R}$ subunits. Nucleofected cortical neurons expressing GABA$_A$Rs (5 DIV) incorporating either $^{M}\beta3$ or $^{M}\beta3^{K12R}$ subunits were biotinylated with NHS-SS-Biotin and lysed. Equal amounts of solubilized protein were added to immobilized avidin and subjected to immunoblotting with anti-myc IgGs. Band intensities were measured, and the data for $^{M}\beta3$ were given a value of 100%. $^{*}p < 0.05$, significantly different from control (*t* test; $n = 4$). Error bars indicate $\pm$ SEM. ***C***, GABA$_A$Rs incorporating $^{M}\beta3$ or $^{M}\beta3^{K12R}$ subunits show similar levels of endocytosis. Transfected neurons were biotinylated with NHS-SS-Biotin and incubated at 37°C for 15 min to allow endocytosis. Biotinylated proteins were purified on immobilized avidin and immunoblotted with anti-myc IgGs. The level of internalized (In) protein at 15 min was then measured and expressed as a percentage of total cell surface (T) at time 0. Error bars indicate $\pm$ SEM ($n = 3$). ***D***, Cell surface GABA$_A$Rs incorporating $^{M}\beta3$ or $^{M}\beta3^{K12R}$ subunits are degraded at a similar rate. Transfected neurons were biotinylated using NHS-SS-Biotin and incubated for 10 h at 37°C. Biotinylated proteins were isolated using immobilized avidin and immunoblotted with anti-myc IgGs, as shown in the top. Band intensities were measured and used to calculate the level of remaining biotinylated $^{M}\beta3$ or $^{M}\beta3$ subunits after 10 h incubation at 37°C, with data seen at time 0 being given a value of 100%. Error bars represent $\pm$ SEM ($n = 3$).

and $^{BBS}\beta3^{K12R}$, with this time point being given a value of 100%. This revealed that GABA$_A$Rs containing $^{BBS}\beta3^{K12R}$ subunits exhibited a significantly higher level of insertion (to 141.6 $\pm$ 15.8% of control) (Fig. 7*B*) compared with those incorporating $^{BBS}\beta3$ subunits

We next used fluorescence imaging in neurons to examine the insertion of GABA$_A$Rs containing either $^{BBS}\beta3$ or $^{BBS}\beta3^{K12R}$ subunits. Nucleofected hippocampal neurons expressing $^{BBS}\beta3$ or $^{BBS}\beta3^{K12R}$ were incubated with Rd–Bgt to label existing populations of receptors containing BBS binding sites. After washing, neurons were incubated with Alx–Bgt for 5 min at 37°C to label newly inserted receptors. Neurons expressing pH–BBS-tagged GABA$_A$R subunits were identified by their endogenous fluorescence attributable to the presence of the pHluorin reporter in these constructs (Fig. 7*C*). Abundant levels of Rd–Bgt labeling were evident only in neurons that also exhibited green fluorescence, and therefore Rd–Bgt staining represents existing cell surface populations of GABA$_A$R at time 0 (Fig. 7*C*). Consistent with our observations in HEK-293 cells, newly inserted receptors (Alx–Bgt staining) were evident after 5 min at 37°C (Fig. 7*C*). The appearance of these new Bgt binding sites could be totally abolished by coincubation with 20 μg/ml unlabeled Bgt (data not shown) (Bogdanov et al., 2006). Proximal dendrites in acquired images were outlined in MetaMorph to determine the average cell surface fluorescence intensity of newly inserted Alx–Bgt-labeled GABA$_A$Rs along 20 μm of a given dendrite. Three dendrites were analyzed per expressing neuron, and at least 15 neurons were examined per construct. By calculating the average fluorescence intensity of Alx–Bgt labeling, it was evident that GABA$_A$Rs incorporating $^{BBS}\beta3^{K12R}$ subunits exhibited significantly higher levels of insertion compared with those incorporating $^{BBS}\beta3$ subunits (to134.7 $\pm$ 8.6% of control) (Fig. 7*D*).

Collectively, these experiments demonstrate that ubiquitination of the GABA$_A$R $\beta3$ subunit acts to regulate receptor insertion primarily from the secretory pathway.

The effects of neuronal activity on GABA$_A$R cell surface expression levels are mediated via $\beta3$ subunit ubiquitination

We examined whether TTX mediates its effects on GABA$_A$R cell surface stability via modulation of $\beta3$ subunit ubiquitination. To do so, we measured the insertion of GABA$_A$Rs containing $^{BBS}\beta3$ and $^{BBS}\beta3^{K12R}$ subunits into the plasma membranes of hippocampal neurons in the presence or absence of TTX using Bgt binding as outlined above. Interestingly, neurons expressing GABA$_A$Rs incorporating $^{BBS}\beta3$ subunits appeared to show reduced levels of Alx–Bgt staining after treatment with TTX compared with those containing $^{BBS}\beta3^{K12R}$ (Fig. 8*A*). Quantifying these data, it was evident that TTX decreased the level of insertion for GABA$_A$Rs containing $^{BBS}\beta3$ by 34 $\pm$ 8% relative to control, but this effect was not replicated for receptors containing $^{pHBBS}\beta3^{K12R}$ subunits (Fig. 8*B*).

Together these results provide a molecular mechanism linking the level of neuronal activity and GABA$_A$R cell surface stability, a mechanism dependent on direct modulation of $\beta3$ subunit ubiquitination, modified proteasomal degradation, and altered rates of plasma membrane insertion.

Chronic blockade of neuronal activity regulates the accumulation of GABA$_A$Rs containing $\beta3$ subunits at synaptic sites

As a final series of experiments, we measured the effects of modulating the level of GABA$_A$R ubiquitination on their accumulation at synapses. Neurons were transfected with $^{BBS}\beta3$ or $^{BBS}\beta^{K12R}$ using nucleofection. At 15 d *in vitro*, neurons were fixed and immunostained with anti-GFP antibodies and with antibodies against synapsin, an accepted marker for presynaptic terminals, followed by confocal microscopy.

The accumulation of $^{BBS}\beta3$ and $^{BBS}\beta^{K12R}$ at synaptic sites was compared using immunofluorescence with an anti-GFP antibody under nonpermeabilized conditions to measure only cell surface receptor populations, followed by anti-synapsin antibodies after permeabilization (Fig. 9*A*). The number of synapses containing recombinant $\beta3$ subunits per unit length of dendrite and their relative intensity were then determined using MetaMorph. From this analysis, it was evident that similar numbers of synapses containing $^{BBS}\beta3$ and $^{BBS}\beta3^{K12R}$ subunits were present on neuronal processes (Fig. 9*B*). However, the intensity of the fluorescence signal for synapses containing $^{BBS}\beta3^{K12R}$ was significantly higher (126.9 $\pm$ 8.4%) compared with synaptic $^{BBS}\beta3$ subunits (Fig. 9*B*). Thus, these results suggest that decreasing GABA$_A$R ubiquitination increases the recep-

tor number at synaptic sites, consistent with their increased cell surface expression levels.

The effects of TTX treatment on the accumulation of $GABA_A$Rs containing recombinant $\beta3$ subunits at synaptic sites was also ascertained using immunofluorescence (Fig. 9*A*). A 24 h, treatment with 2 μM TTX significantly decreased the number of synaptic sites containing $^{BBS}\beta3$ from 17.6 ± 1.9 per 50 μm of dendrite in control compared with 8.6 ± 1.1 in the presence of this agent (Fig. 9*C*). In contrast, TTX did not significantly alter the number of synapses containing $^{BBS}\beta3^{K12R}$ subunits (Fig. 9*C*). In addition, TTX also reduced the intensity of $^{BBS}\beta3$ staining at remaining synapses by 31.8 ± 3.5% relative to control, an effect not replicated for synapses containing $^{BBS}\beta3^{K12R}$ subunits (Fig. 9*D*).

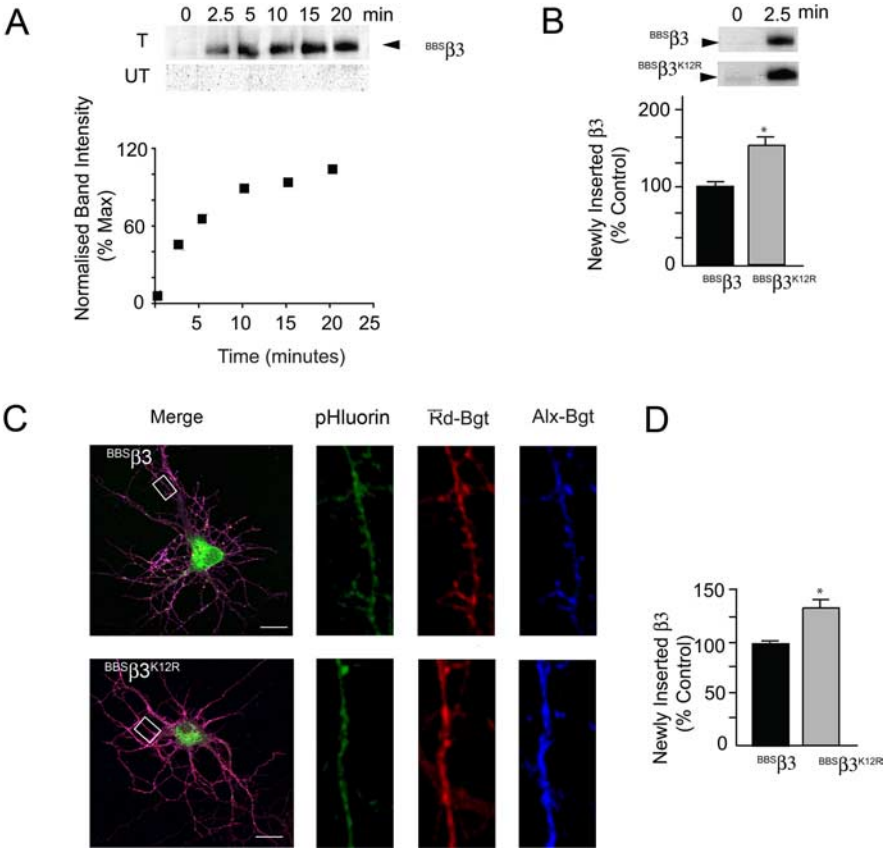

Figure 7. $GABA_A$Rs incorporating $\beta3^{K12R}$ subunits exhibit enhanced insertion into the plasma membrane. ***A***, Time-dependent membrane insertion of $GABA_A$Rs in HEK-293 cells. Cells expressing receptor $\alpha1^{BBS}\beta3$ subunits or untransfected (UT) controls were exposed to 10 μg/ml α-Bgt to block existing surface receptors. Cells were then washed in PBS before incubation with 10 μg/ml biotinylated-Bgt at 37°C for varying time periods, as shown. After lysis, biotinylated Bgt-labeled $^{BBS}\beta3$ subunits were isolated on immobilized avidin and immunoblotted with anti-GFP antibodies as shown in the top. Band intensities were measured and used to calculate the insertion rate of receptors. Band intensities were normalized to the maximum band intensity at 20 min. T, Total cell surface. ***B***, Enhanced membrane insertion of $GABA_A$Rs containing $^{BBS}\beta3^{K12R}$ subunits. HEK-293 cells expressing $GABA_A$Rs composed of $\alpha1^{BBS}\beta3$ or $\alpha1^{BBS}\beta3^{K12R}$ subunits were treated as outlined in ***A***, and receptor $\beta3$ subunits were visualized by immunoblotting as shown in the top. These data were then used to compare the levels of receptor insertion at 2.5 min, with data being normalized to the value for $^{BBS}\beta3$ (control) subunits. *$p < 0.05$, significantly different from control (unpaired *t* test; $n = 5$). Error bars represent ± SEM. ***C***, Imaging the insertion of $GABA_A$Rs in hippocampal neurons. Neurons (15 DIV) expressing $GABA_A$R $^{BBS}\beta3$ or $^{BBS}\beta3^{K12R}$ subunits were labeled at 37°C with 10 μg/ml Rd–Bgt for 15 min, washed before incubation with 10 μg/ml Alx–Bgt for 5 min at 37°C, and then fixed. Images of pHluorin fluorescence and Rd–Bgt and Alx–Bgt staining, as indicated, were then recorded using confocal microscopy. Boxed areas outlined in image of neurons expressing $^{BBS}\beta3$ or $^{BBS}\beta3^{K12R}$ are magnified in panels on the right. Scale bars, 10 μm. ***D***, Quantification of cell surface fluorescence intensity of newly inserted Alx–Bgt-labeled $GABA_A$Rs. Data were normalized to values seen in neurons expressing receptor $^{BBS}\beta3$ subunits (control). *$p < 0.05$, significantly different from control (unpaired *t* test; $n = 15$). Error bars represent ± SEM.

Discussion

We have begun to assess the role that chronic changes in neuronal activity play in determining the membrane trafficking and synaptic accumulation of $GABA_A$Rs. We demonstrated that blockade of neuronal depolarization with TTX or the activity of ionotropic glutamate receptors for 24 h decreased the cell surface stability of $GABA_A$Rs receptors containing $\beta3$, $\alpha2$, or $\gamma2$ subunits; in contrast, enhancing neuronal activity increases the accumulation of these proteins on the neuronal plasma membrane. Therefore, these combined experiments suggest that the level of neuron activity is a powerful determinant of the number of $GABA_A$Rs subtypes containing $\beta3$, $\alpha2$, or $\gamma2$ on the plasma membrane of cultured cortical and hippocampal neurons. Previous studies on the role that neuronal activity plays in regulating $GABA_A$R cell surface stability have proven controversial. Electrophysiological approaches in mature cultured cortical neurons have shown that chronic inactivity decreases $GABA_A$R number and reduces both frequency and amplitude of miniature inhibitory synaptic currents (Turrigiano et al., 1998; Kilman et al., 2002). In contrast, blockade of synaptic activity in developing hippocampal neurons does not appear to modify the number of cell surface $GABA_A$Rs or their accumulation at synaptic sites (Harms and Craig, 2005). This discrepancy may reflect the varying ages of the culture preparations used (Huupponen et al., 2007) or the length of activity blockade, 24 h compared with 18 d. Intriguingly, it has been demonstrated recently that exposure of cultured neurons to TTX over a period of 7–14 d results in retraction of dendrites and a loss of spines (Fishbein and Segal, 2007). Therefore, this phenomenon may complicate the analysis of the long-term effects of activity blockade on the formation of inhibitory synapses.

In addition to decreasing cell surface expression levels, TTX treatment dramatically enhanced the ubiquitination of the $GABA_A$R $\beta3$ subunit over the same time course. Accordingly, the ability of TTX to decrease $GABA_A$R cell surface expression levels was dependent on the activity of the proteasome. Interestingly, enhancing neuronal activity by pharmacological blockade of $GABA_A$Rs resulted in decreased receptor ubiquitination and enhanced cell surface expression levels. TTX treatment did not alter receptor endocytosis or cell surface half-life, suggesting that neuronal activity primarily acts to regulate receptor insertion into the plasma membrane from the secretory pathway. Consistent with this, pulse-chase analysis revealed that TTX reduced the stability of newly translated receptor subunits primarily in the ER, the principal subcellular site of $GABA_A$R assembly (Gorrie et al., 1997; Bedford et al., 2001). Thus, these results suggest that the level of neuronal activity is a key determinant of $GABA_A$R cell surface stability and strongly suggest that these effects are mediated by altered receptor ubiquitination and proteasomal degra-

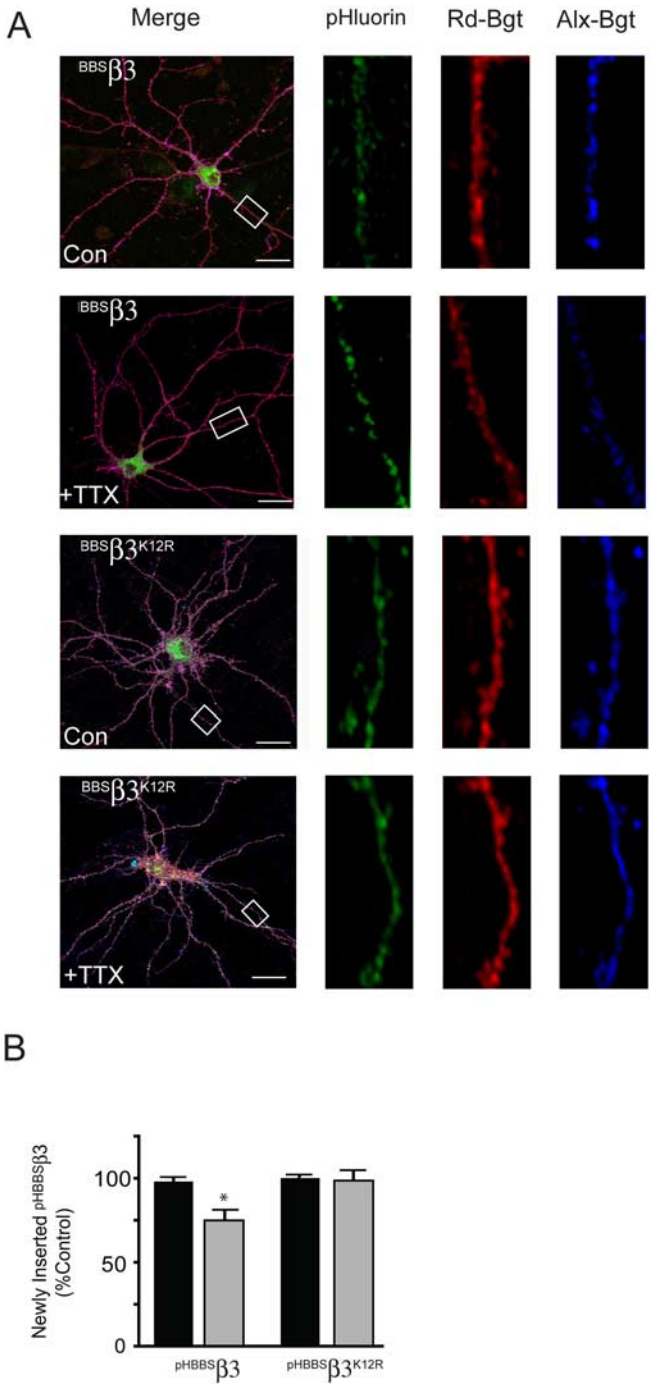

Figure 8. Neuronal activity blockade modulates the membrane insertion of $GABA_A$Rs incorporating $^{BBS}\beta3$ subunits but not $^{BBS}\beta3^{K12R}$ subunits. ***A***, Hippocampal neurons (15 DIV) expressing either $GABA_A$R $^{BBS}\beta3$ or $^{BBS}\beta3^{K12R}$ subunits were treated with or without TTX, as indicated, for 24 h. Neurons were incubated with 10 μg/ml Rd–Bgt to label existing $^{BBS}\beta3$ or $^{BBS}\beta3^{K12R}$, washed, incubated for 5 min with 10 μg/ml Alx–Bgt to label newly inserted $^{BBS}\beta3$ and $^{BBS}\beta3^{K12R}$ subunits, and then fixed. Images of pHluorin fluorescence and Rd–Bgt and Alx–Bgt staining, as indicated, were recorded using confocal microscopy. Boxed areas outlined in image of neurons expressing $^{BBS}\beta3$ or $^{BBS}\beta3^{K12R}$ are magnified in panels on the right. Con, Control. ***B***, Quantification of Alx–Bgt fluorescence intensity. Dendrites in acquired images were outlined in MetaMorph to determine cell surface fluorescence intensity of newly inserted Alx–Bgt-labeled $^{BBS}\beta3$ and $^{BBS}\beta3^{K12R}$ in the presence (gray bars) or absence (black bars) of TTX. Three dendrites (20 μm) were analyzed per neuron, and at least 15 neurons were examined per construct. Data were then normalized to values seen in control neurons expressing $GABA_A$R $^{BBS}\beta3$ or $^{BBS}\beta3^{K12R}$ subunits. *$p < 0.05$, significantly different from control (t test; $n = 15$). Error bars represent ± SEM.

dation of the NMDA receptor subunit NR1 has been observed in hippocampal neurons (Kato et al., 2005). However, activity-dependent ubiquitination of mammalian AMPA receptor subunits has not been demonstrated, although chronic changes in activity regulate the ubiquitination and turnover of associated postsynaptic density proteins (Colledge et al., 2003; Patrick et al., 2003). In contrast, ubiquitination has been illustrated to regulate the endocytosis of AMPA receptors in *Caenorhabditis elegans* (Burbea et al., 2002).

To further explore the significance of activity-dependent ubiquitination, we used mutagenesis to convert all 12 lysine residues ($\beta3^{K12R}$) within the major intracellular domain of the $GABA_A$R $\beta3$ subunit to arginines. These mutations significantly reduced $\beta3$ subunit ubiquitination but did not compromise assembly with the $\alpha1$ and $\gamma2$ subunits into functional benzodiazepine-sensitive heteromeric $GABA_A$Rs. Significantly higher levels of cell surface expression of the $\beta3^{K12R}$ mutant were evident compared with wild-type subunits in both expression systems and neurons. These mutations did not alter $GABA_A$Rs endocytosis or cell surface stability but significantly enhanced receptor insertion into the plasma membrane. Collectively, these experiments together with our pulse-chase analysis suggest that ubiquitination of the $\beta3$ subunit primarily acts to regulate subunit stability within the ER. Consistent with this, it is well established that polyubiquitination is required for retrotranslocation of proteins from the endoplasmic reticulum back into the cytosol, in which they are degraded by the proteasome (Ye et al., 2003). Given the critical role that receptor β subunits play in regulating the ER exit of assembled $GABA_A$Rs (Luscher and Keller, 2004), this reduced level of $\beta3$ subunits would be predicted to reduce the pool of fully assembled heteromeric receptors for insertion into the plasma membrane. In support of this idea, previous studies have shown that blocking ER-associated degradation of nicotinic acetylcholine receptors with proteasome inhibitors leads to increased receptor ubiquitination and also subunit oligomerization, which resulted in increased receptor insertion into the plasma membrane (Christianson and Green, 2004).

To directly test role that activity-dependent ubiquitination plays in regulating the accumulation of $GABA_A$R at synaptic sites, we used $\beta3$ subunit expression constructs modified with N-terminal extracellular pHluorin and BBS reporters (Bogdanov et al., 2006). Using imaging with fluorescent Bgt, this approach demonstrated that $GABA_A$Rs incorporating $\beta3^{K12R}$ subunits showed significantly higher rates of insertion into the plasma membrane compared with their wild-type equivalents. In agreement with this, higher levels of accumulation of $GABA_A$Rs containing $^{BBS}\beta3^{K12R}$ subunits were evident at synapses compared with those containing wild-type $^{BBS}\beta3$. Moreover, TTX treatment significantly reduced the number of synapses containing $^{BBS}\beta3$ subunits together with receptor number at remaining synapses. However, the synaptic accumulation of receptors containing $^{BBS}\beta3^{K12R}$ was unaffected by TTX treatment. Therefore, these studies strongly suggest that neuronal activity can modulate the accumulation of $GABA_A$Rs at synaptic sites via regulating the ubiquitination of these proteins in the secretory pathway and their subsequent insertion into the plasma membrane.

The molecular details of how altered levels of neuronal activity regulate $GABA_A$R ubiquitination remain to be established but are likely to be highly dynamic and determined by the activity of individual ubiquitin-ligase/hydrolyases and other modulators of proteasomal degradation. It should be noted that $GABA_A$Rs bind directly to the ubiquitin-like protein Plic-1 (Bedford et al., 2001), an established regulator of ubiquitin-dependent proteasomal

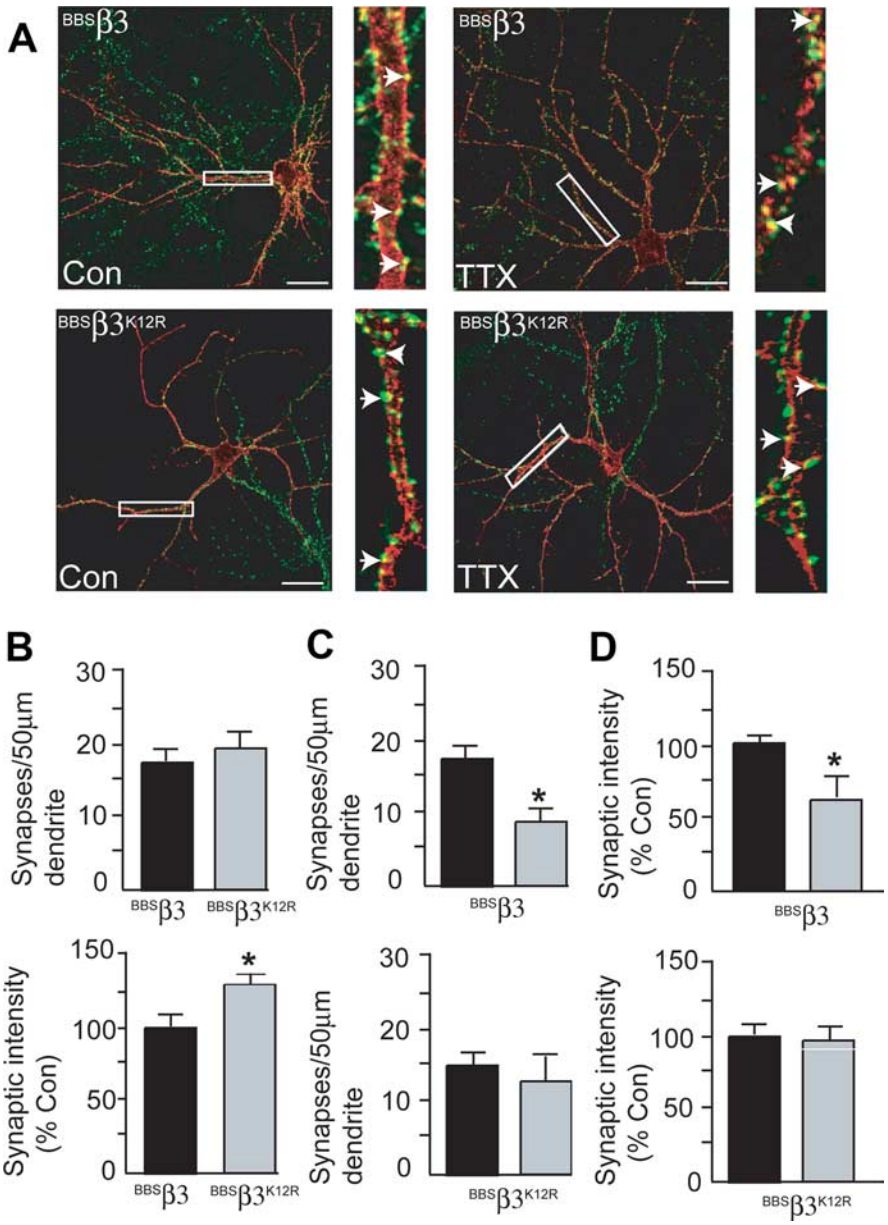

Figure 9. Activity blockade regulates the accumulation of $GABA_A$Rs, containing the $^{BBS}\beta3$ subunit but not the $^{BBS}\beta3^{K12R}$ subunit at synaptic sites. ***A***, Images of hippocampal neurons (15 DIV) expressing $GABA_A$R $^{BBS}\beta3$ or $^{BBS}\beta3^{K12R}$ subunits treated with or without TTX (2 μM) for 24 h, as indicated. Neurons were fixed and stained with rabbit anti-GFP IgGs and Texas Red-conjugated anti-rabbit IgGs. Neurons were then permeabilized and stained with monoclonal anti-synapsin IgGs and Cy5-conjugated anti-mouse IgGs (synapsin staining was assigned the color green). Panels on the right in each image represent enlargements of the boxed areas outlined in the left panels, and arrows indicate synaptic sites containing $^{BBS}\beta3$ or $^{BBS}\beta3^{K12R}$. Scale bars, 10 μm. ***B***, Quantification of the number of $^{BBS}\beta3$ and $^{BBS}\beta3^{K12R}$ synaptic sites and their fluorescence intensity. Synaptic sites were defined by the colocalization of anti-GFP staining with synapsin staining for $GABA_A$Rs incorporating either $^{BBS}\beta3$ or $^{BBS}\beta3^{K12R}$ subunits. *$p < 0.05$, significantly different from $^{BBS}\beta3$ (unpaired *t* test; $n = 20$ neurons). ***C***, Quantification of the number of $^{BBS}\beta3$ and $^{BBS}\beta3^{K12R}$ synaptic sites after incubation with (gray bars) or without (black bars) TTX (*$p < 0.05$, significantly different from control, *t* test; $n = 15$–20 neurons). ***D***, Quantification of $^{BBS}\beta3$ and $^{BBS}\beta3^{K12R}$ subunit fluorescence intensity at synaptic sites. The intensity of Texas Red fluorescence colocalizing with 0.5–2 μm areas containing synapsin staining were determined for neurons expressing $^{BBS}\beta3$ or $^{BBS}\beta3^{K12R}$ subunits under control conditions (black bars) or after treatment with TTX (black bars). Average fluorescence intensity data in control neurons were assigned a value of 100% (black bars). *$p <$ 0.05, significantly different from control (*t* test; $n = 15$–20 neurons). Error bars throughout represent $\pm$ SEM. Con, Control.

degradation, further highlighting a possible mechanism neurons may use to control $GABA_A$R ubiquitination. In addition to controlling the stability of $GABA_A$Rs, neuronal activity may also regulate the formation of inhibitory synapses at many additional loci, ranging from the stability of cytoskeletal anchors such as gephyrin to the number of innervating presynaptic terminals (Craig et al., 2006).

In summary, our results provide evidence that neuronal activity can regulate the number of cell surface $GABA_A$Rs by modulating their ubiquitination and subsequent proteasomal degradation in the secretory pathway. This process can directly regulate the level of $GABA_A$R insertion into the plasma membrane and their subsequent accumulation at postsynaptic sites. This putative mechanism may therefore play a critical role in coordinating the level of local synaptic activity in the brain and thus contribute to homeostatic synaptic plasticity.

References

Bedford FK, Kittler JT, Muller E, Thomas P, Uren JM, Merlo D, Wisden W, Triller A, Smart TG, Moss SJ (2001) GABA(A) receptor cell surface number and subunit stability are regulated by the ubiquitin-like protein Plic-1. Nat Neurosci 4:908–916.

Bogdanov Y, Michels G, Armstrong-Gold C, Haydon PG, Lindstrom J, Pangalos M, Moss SJ (2006) Synaptic GABAA receptors are directly recruited from their extrasynaptic counterparts. EMBO J 25:4381–4389.

Brandon NJ, Delmas P, Kittler JT, McDonald BJ, Sieghart W, Brown DA, Smart TG, Moss SJ (2000) GABAA receptor phosphorylation and functional modulation in cortical neurons by a protein kinase C-dependent pathway. J Biol Chem 275:38856–38862.

Brandon NJ, Delmas P, Hill J, Smart TG, Moss SJ (2001) Constitutive tyrosine phosphorylation of the GABA(A) receptor gamma 2 subunit in rat brain. Neuropharmacology 41:745–752.

Burbea M, Dreier L, Dittman JS, Grunwald ME, Kaplan JM (2002) Ubiquitin and AP180 regulate the abundance of GLR-1 glutamate receptors at postsynaptic elements in *C. elegans*. Neuron 35:107–120.

Chen G, Kittler JT, Moss SJ, Yan Z (2006) Dopamine D_3 receptors regulate GABAA receptor function through a phospho-dependent endocytosis mechanism in nucleus accumbens. J Neurosci 26:2513–2521.

Christianson JC, Green WN (2004) Regulation of nicotinic receptor expression by the ubiquitin-proteasome system. EMBO J 23:4156–4165.

Colledge M, Snyder EM, Crozier RA, Soderling JA, Jin Y, Langeberg LK, Lu H, Bear MF, Scott JD (2003) Ubiquitination regulates PSD-95 degradation and AMPA receptor surface expression. Neuron 40:595–607.

Connolly CN, Wooltorton JR, Smart TG, Moss SJ (1996) Subcellular localization of gamma-aminobutyric acid type A receptors is determined by receptor beta subunits. Proc Natl Acad Sci USA 93:9899–9904.

Couve A, Restituito S, Brandon JM, Charles KJ, Bawagan H, Freeman KB, Pangalos MN, Calver AR, Moss SJ (2004) Marlin-1, a novel RNA-binding protein associates with GABA receptors. J Biol Chem 279:13934–13943.

Craig AM, Graf ER, Linhoff MW (2006) How to build a central synapse: clues from cell culture. Trends Neurosci 29:8–20.

Essrich C, Lorez M, Benson JA, Fritschy JM, Luscher B (1998) Postsynaptic

clustering of major GABAA receptor subtypes requires the gamma 2 subunit and gephyrin. Nat Neurosci 1:563–571.

Fishbein I, Segal M (2007) Miniature synaptic currents become neurotoxic to chronically silenced neurons. Cereb Cortex 17:1292–1306.

Fiumelli H, Cancedda L, Poo MM (2005) Modulation of GABAergic transmission by activity via postsynaptic Ca^{2+}-dependent regulation of KCC2 function. Neuron 48:773–786.

Fritschy JM, Mohler H (1995) GABAA-receptor heterogeneity in the adult rat brain: differential regional and cellular distribution of seven major subunits. J Comp Neurol 359:154–194.

Glickman MH, Ciechanover A (2002) The ubiquitin-proteasome proteolytic pathway: destruction for the sake of construction. Physiol Rev 82:373–428.

Gorrie GH, Vallis Y, Stephenson A, Whitfield J, Browning B, Smart TG, Moss SJ (1997) Assembly of GABAA receptors composed of alpha1 and beta2 subunits in both cultured neurons and fibroblasts. J Neurosci 17:6587–6596.

Haglund K, Dikic I (2005) Ubiquitylation and cell signaling. EMBO J 24:3353–3359.

Haglund K, Di Fiore PP, Dikic I (2003a) Distinct monoubiquitin signals in receptor endocytosis. Trends Biochem Sci 28:598–603.

Haglund K, Sigismund S, Polo S, Szymkiewicz I, Di Fiore PP, Dikic I (2003b) Multiple monoubiquitination of RTKs is sufficient for their endocytosis and degradation. Nat Cell Biol 5:461–466.

Harms KJ, Craig AM (2005) Synapse composition and organization following chronic activity blockade in cultured hippocampal neurons. J Comp Neurol 490:72–84.

Hartman KN, Pal SK, Burrone J, Murthy VN (2006) Activity-dependent regulation of inhibitory synaptic transmission in hippocampal neurons. Nat Neurosci 9:642–649.

Homanics GE, DeLorey TM, Firestone LL, Quinlan JJ, Handforth A, Harrison NL, Krasowski MD, Rick CE, Korpi ER, Makela R, Brilliant MH, Hagiwara N, Ferguson C, Snyder K, Olsen RW (1997) Mice devoid of gamma-aminobutyrate type A receptor beta3 subunit have epilepsy, cleft palate, and hypersensitive behavior. Proc Natl Acad Sci USA 94:4143–4148.

Huupponen J, Molchanova SM, Taira T, Lauri SE (2007) Susceptibility for homeostatic plasticity is down-regulated in parallel with maturation of the rat hippocampal synaptic circuitry. J Physiol (Lond) 581:505–514.

Jacob TC, Bogdanov YD, Magnus C, Saliba RS, Kittler JT, Haydon PG, Moss SJ (2005) Gephyrin regulates the cell surface dynamics of synaptic $GABA_A$ receptors. J Neurosci 25:10469–10478.

Jovanovic JN, Thomas P, Kittler JT, Smart TG, Moss SJ (2004) Brain-derived neurotrophic factor modulates fast synaptic inhibition by regulating $GABA_A$ receptor phosphorylation, activity, and cell-surface stability. J Neurosci 24:522–530.

Katchalski-Katzir E, Kasher R, Balass M, Scherf T, Harel M, Fridkin M, Sussman JL, Fuchs S (2003) Design and synthesis of peptides that bind alpha-bungarotoxin with high affinity and mimic the three-dimensional structure of the binding-site of acetylcholine receptor. Biophys Chem 100:293–305.

Kato A, Rouach N, Nicoll RA, Bredt DS (2005) Activity-dependent NMDA receptor degradation mediated by retrotranslocation and ubiquitination. Proc Natl Acad Sci USA 102:5600–5605.

Kilman V, van Rossum MC, Turrigiano GG (2002) Activity deprivation reduces miniature IPSC amplitude by decreasing the number of postsynaptic $GABA_A$ receptors clustered at neocortical synapses. J Neurosci 22:1328–1337.

Kittler JT, Moss SJ (2003) Modulation of GABAA receptor activity by phosphorylation and receptor trafficking: implications for the efficacy of synaptic inhibition. Curr Opin Neurobiol 13:341–347.

Kittler JT, Delmas P, Jovanovic JN, Brown DA, Smart TG, Moss SJ (2000) Constitutive endocytosis of GABAA receptors by an association with the adaptin AP2 complex modulates inhibitory synaptic currents in hippocampal neurons. J Neurosci 20:7972–7977.

Kittler JT, Thomas P, Tretter V, Bogdanov YD, Haucke V, Smart TG, Moss SJ (2004) Huntingtin-associated protein 1 regulates inhibitory synaptic transmission by modulating gamma-aminobutyric acid type A receptor membrane trafficking. Proc Natl Acad Sci USA 101:12736–12741.

Kittler JT, Chen G, Honing S, Bogdanov Y, McAinsh K, Arancibia-Carcamo IL, Jovanovic JN, Pangalos MN, Haucke V, Yan Z, Moss SJ (2005) Phospho-dependent binding of the clathrin AP2 adaptor complex to GABAA receptors regulates the efficacy of inhibitory synaptic transmission. Proc Natl Acad Sci USA 102:14871–14876.

Luscher B, Keller CA (2004) Regulation of GABAA receptor trafficking, channel activity, and functional plasticity of inhibitory synapses. Pharmacol Ther 102:195–221.

Mohler H, Fritschy JM, Vogt K, Crestani F, Rudolph U (2005) Pathophysiology and pharmacology of GABA(A) receptors. Handb Exp Pharmacol 225–247.

O'Brien RJ, Kamboj S, Ehlers MD, Rosen KR, Fischbach GD, Huganir RL (1998) Activity-dependent modulation of synaptic AMPA receptor accumulation. Neuron 21:1067–1078.

Patrick GN, Bingol B, Weld HA, Schuman EM (2003) Ubiquitin-mediated proteasome activity is required for agonist-induced endocytosis of GluRs. Curr Biol 13:2073–2081.

Rao A, Craig AM (1997) Activity regulates the synaptic localization of the NMDA receptor in hippocampal neurons. Neuron 19:801–812.

Rudolph U, Mohler H (2004) Analysis of GABAA receptor function and dissection of the pharmacology of benzodiazepines and general anesthetics through mouse genetics. Annu Rev Pharmacol Toxicol 44:475–498.

Rudolph U, Mohler H (2006) GABA-based therapeutic approaches: GABAA receptor subtype functions. Curr Opin Pharmacol 6:18–23.

Rutherford LC, DeWan A, Lauer HM, Turrigiano GG (1997) Brain-derived neurotrophic factor mediates the activity-dependent regulation of inhibition in neocortical cultures. J Neurosci 17:4527–4535.

Scherf T, Kasher R, Balass M, Fridkin M, Fuchs S, Katchalski-Katzir E (2001) A beta-hairpin structure in a 13-mer peptide that binds alpha -bungarotoxin with high affinity and neutralizes its toxicity. Proc Natl Acad Sci USA 98:6629–6634.

Sekine-Aizawa Y, Huganir RL (2004) Imaging of receptor trafficking by using alpha-bungarotoxin-binding-site-tagged receptors. Proc Natl Acad Sci USA 101:17114–17119.

Sieghart W, Sperk G (2002) Subunit composition, distribution and function of GABA(A) receptor subtypes. Curr Top Med Chem 2:795–816.

Taylor PM, Thomas P, Gorrie GH, Connolly CN, Smart TG, Moss SJ (1999) Identification of amino acid residues within $GABA_A$ receptor beta subunits that mediate both homomeric and heteromeric receptor expression. J Neurosci 19:6360–6371.

Taylor PM, Connolly CN, Kittler JT, Gorrie GH, Hosie A, Smart TG, Moss SJ (2000) Identification of residues within $GABA_A$ receptor α subunits that mediate specific assembly with receptor β subunits. J Neurosci 20:1297–1306.

Turrigiano GG, Leslie KR, Desai NS, Rutherford LC, Nelson SB (1998) Activity-dependent scaling of quantal amplitude in neocortical neurons. Nature 391:892–896.

Woodin MA, Ganguly K, Poo MM (2003) Coincident pre- and postsynaptic activity modifies GABAergic synapses by postsynaptic changes in Cl^- transporter activity. Neuron 39:807–820.

Wooltorton JR, Moss SJ, Smart TG (1997) Pharmacological and physiological characterization of murine homomeric beta3 GABA(A) receptors. Eur J Neurosci 9:2225–2235.

Ye Y, Meyer HH, Rapoport TA (2003) Function of the p97-Ufd1-Npl4 complex in retrotranslocation from the ER to the cytosol: dual recognition of nonubiquitinated polypeptide segments and polyubiquitin chains. J Cell Biol 162:71–84.